12-17-2013

A Pil1–Sle1–Syj1–Tax4 Functional Pathway Links Eisosomes with PI(4,5)P2 Regulation

Ruth Kabeche
Dartmouth College

Assen Roguev
University of California, San Francisco

Nevan J. Krogan
University of California, San Francisco

James B. Moseley
Dartmouth College

© 2014. Published by The Company of Biologists Ltd | Journal of Cell Science (2014) 127, 1318–1326 doi:10.1242/jcs.143545

RESEARCH ARTICLE

A Pil1–Sle1–Syj1–Tax4 functional pathway links eisosomes with PI(4,5)P_2 regulation

Ruth Kabeche[1], Assen Roguev[2,3], Nevan J. Krogan[2,3,4] and James B. Moseley[1,*]

ABSTRACT

Stable compartments of the plasma membrane promote a wide range of cellular functions. In yeast cells, cytosolic structures called eisosomes generate prominent cortical invaginations of unknown function. Through a series of genetic screens in fission yeast, we found that the eisosome proteins Pil1 and Sle1 function with the synaptojanin-like lipid phosphatase Syj1 and its ligand Tax4. This genetic pathway connects eisosome function with the hydrolysis of phosphatidylinositol (4,5)-bisphosphate [PI(4,5)P_2] in cells. Defects in PI(4,5)P_2 regulation led to eisosome defects, and we found that the core eisosome protein Pil1 can bind to and tubulate liposomes containing PI(4,5)P_2. Mutations in components of the Pil1–Sle1–Syj1–Tax4 pathway suppress the growth and morphology defects of TORC2 mutants, indicating that eisosome-dependent regulation of PI(4,5)P_2 feeds into signal transduction pathways. We propose that the geometry of membrane invaginations generates spatial and temporal signals for lipid-mediated signaling events in cells.

KEY WORDS: Eisosome, PI(4,5)P_2, Synaptojanin, TORC2

INTRODUCTION

A defining feature of eukaryotic cells is the presence of discrete intracellular structures that compartmentalize the chemical reactions underlying cellular physiology. A long-standing goal of cell biology research is to identify these structures and then to define their functional links to cellular processes. At the plasma membrane, cellular structures compartmentalize cortical lipids to ensure the fidelity and efficiency of different functions such as signal transduction, endocytosis and polarized growth (Hartman and Groves, 2011; Lingwood and Simons, 2010; Olivera-Couto and Aguilar, 2012; Ziółkowska et al., 2011). These compartments and microdomains have the potential to span a wide range of spatial and temporal scales tailored for discrete cellular functions.

The yeast plasma membrane has served as a model system for identifying the mechanisms and functions of cortical compartmentalization (Ziółkowska et al., 2012). In yeast cells, a prominent cortical microdomain, often called the MCC (for membrane compartment occupied by Can1), appears as a series of linear invaginations that extend approximately 200 nm in budding yeast cells and 1–2 µm in fission yeast cells (Grossmann et al., 2008; Grossmann et al., 2007; Kabeche et al., 2011; Malinska et al., 2004; Moreira et al., 2009; Snaith et al., 2011; Strádalová et al., 2009; Young et al., 2002). These cortical microdomains are formed by a cellular structure termed the eisosome (Walther et al., 2006). The highly abundant Bin–Amphiphysin–Rvs (BAR)-domain protein Pil1 is the core component of eisosomes (Grossmann et al., 2007; Olivera-Couto et al., 2011; Walther et al., 2006; Ziółkowska et al., 2011). Pil1 is present at ~100,000 copies per budding yeast cell and is found at similar levels in fission yeast (Marguerat et al., 2012; Walther et al., 2006). Each eisosome contains thousands of copies of Pil1, which can self-assemble into linear tubules and can also generate lipid tubules *in vitro* (Kabeche et al., 2011; Karotki et al., 2011; Olivera-Couto et al., 2011). Eisosomes and Pil1-related proteins appear to be conserved throughout all ascomycete fungi (Douglas et al., 2011; Olivera-Couto and Aguilar, 2012; Scazzocchio et al., 2011; Ziółkowska et al., 2012). Through studies in many species, it appears that Pil1-assembled eisosomes represent an abundant and prominent structure at the cortex of yeast cells.

The cellular function of eisosomes has been enigmatic and controversial. Early studies in budding yeast showed that the MCC/eisosome protein Sur7 was distinct from cortical actin patches, which represent sites of endocytosis (Young et al., 2002). A subsequent study suggested that eisosomes might mark sites of endocytosis at cortical actin patches (Walther et al., 2006), but later work has shown that eisosomes are not linked to endocytosis at actin patches (Brach et al., 2011). In budding yeast cells, many proteins in addition to Pil1 localize at MCC/eisosomes (Fröhlich et al., 2009; Grossmann et al., 2008). By contrast, fission yeast eisosomes contain only two additional proteins: the transmembrane protein Fhn1 and the peripheral membrane protein Sle1, which are both required for proper eisosome formation in cells (Kabeche et al., 2011; Moreira et al., 2012). This suggests that fission yeast eisosomes might represent a simplified form of this prominent cellular structure. To study the function of this conserved and mysterious intracellular structure, we have investigated the simplified eisosome of the fission yeast *Schizosaccharomyces pombe*. Our combined genetic, genomic and biochemical approaches have identified a genetic pathway that links eisosomes to regulation of the phosphoinositide phosphatidylinositol (4,5)-bisphosphate [PI(4,5)P_2.]. Furthermore, this function of eisosomes is connected to signaling by the conserved TORC2 complex, suggesting that eisosomes compartmentalize PI(4,5)P_2 regulation at the plasma membrane to mediate signal transduction pathways in cells.

RESULTS

Identification of a Pil1–Sle1–Syj1–Tax4 functional pathway

We performed a series of genetic screens in fission yeast to identify a genetic pathway for eisosome function (Roguev et al., 2007). Both *pil1Δ* and *sle1Δ* strains were crossed separately with

[1]Department of Biochemistry, Geisel School of Medicine at Dartmouth, Hanover, NH 03755, USA. [2]Department of Cellular and Molecular Pharmacology, University of California, San Francisco, CA 94158, USA. [3]California Institute for Quantitative Biosciences, QB3, San Francisco, CA 94158, USA. [4]J. David Gladstone Institutes, San Francisco, CA 94158, USA.

*Author for correspondence (james.b.moseley@dartmouth.edu)

Received 26 September 2013; Accepted 17 December 2013

Journal of Cell Science

Journal of Cell Science (2014) 127, 1318–1326 doi:10.1242/jcs.143545

an ordered array of ~2,200 non-essential *S. pombe* deletion mutants, and the fitness of the resulting double mutants was assessed. We anticipated that *pil1Δ* and *sle1Δ* mutants would show similar genetic interactions because both Pil1 and Sle1 are required for proper formation of eisosomes in cells. As a control, we also screened a deletion of *pil2+*, which encodes a protein that assembles eisosome-like filaments in meiotic spores, but which is not expressed in mitotic cells (Kabeche et al., 2011). For each screen, we defined mutants that were synthetic sick or synthetic lethal (SS/SL) with *pil1Δ* and *sle1Δ*, indicating overlapping function in cells (supplementary material Table S1). We also defined a set of genes that displayed similar genetic interaction patterns with *pil1Δ* and *sle1Δ* (supplementary material Table S1); such correlated genes often function together (Beltrao et al., 2010; Roguev et al., 2008; Ryan et al., 2012).

In these screens, *pil1Δ* and *sle1Δ* were highly correlated (cc=0.49), consistent with their shared function at eisosomes. Intriguingly, the genetic interaction profiles of both *pil1Δ* and *sle1Δ* were also highly correlated with *syj1Δ* and *tax4Δ* (Fig. 1A). Syj1 (Inp51 in *Saccharomyces cerevisiae*) is a synaptojanin-like polyphosphoinositide phosphatase for PI(4,5)P_2. We note that *pil1Δ* and *inp51Δ* also show similar genetic profiles in budding yeast (Aguilar et al., 2010; Karotki et al., 2011), suggesting that this is a conserved genetic connection. Tax4 (SPAC1687.09, previously uncharacterized) is the sole *S. pombe* ortholog of *S. cerevisiae* Tax4 and Irs4, which bind to a conserved asparagine−proline−phenylalanine (NPF) motif in Syj1(Inp51) and regulate PI(4,5)P_2 hydrolysis (Fig. 1B) (Morales-Johansson et al., 2004). Similar to its budding yeast counterparts, *S. pombe* Tax4 contains an ENTH (epsin N-terminal homology)/VHS (VPS27, Hrs and STAM) domain that is predicted to bind to PI(4,5)P_2. These genetic interactions suggest that Pil1, Sle1, Syj1 and Tax4 function together in a linear pathway. These proteins all have domains that are predicted to bind to PI(4,5)P_2, raising the possibility that they function as a unit in regulating this lipid.

In our genetic screens, *pil1Δ* and *sle1Δ* were synthetically lethal with *inp53Δ*, *whi2Δ* and *arv1Δ* (Fig. 1A). Directed crosses and tetrad dissection confirmed these interactions (Figs 1C; supplementary material Fig. S1A). In addition, both *syj1Δ* and *tax4Δ* were synthetically lethal with *inp53Δ*, *whi2Δ* and *arv1Δ* (Figs 1C; supplementary material Fig. S1A). Synthetic lethality between *inp53Δ* and *pil1Δ* (and *inp53Δ* and *syj1Δ*) is not due to germination defects as double-mutant cells germinate and divide before dying (supplementary material Fig. S1B). Furthermore, correlating mutants *pil1Δ*, *sle1Δ*, *syj1Δ* and *tax4Δ* do not show any synthetic phenotypes with each other (supplementary material Fig. S1C; data not shown). While Whi2 and Arv1 are largely uncharacterized, Inp53 is a 5′ phosphatase for PI(4,5)P_2, similar to Syj1. The synthetic lethality of *syj1Δ* and *inp53Δ* suggests that Syj1 and Inp53 are overlapping phosphatases that act in parallel pathways to regulate PI(4,5)P_2. These genetic data link eisosomes to the hydrolysis of PI(4,5)P_2, with the Pil1–Sle1–Syj1–Tax4 functional pathway operating in parallel to Inp53.

We used the temperature-sensitive *its3-1* mutant to test the connection between eisosomes and PI(4,5)P_2. Its3 is the essential 5′ kinase that converts phosphatidylinositol (4)-phosphate [PI(4)P] to PI(4,5)P_2 (Fig. 2A), and the *its3-1* mutant exhibits decreased levels of PI(4,5)P_2 even at permissive temperatures (Mitra et al., 2004). If mutations in the Pil1–Sle1–Syj1–Tax4 pathway impair the hydrolysis of PI(4,5)P_2 then these mutations are predicted to suppress the *its3-1* mutant. Indeed, we observed partial suppression of *its3-1* lethality when combined with *pil1Δ*, *sle1Δ*, *syj1Δ* or *tax4Δ* (Fig. 2B). A similar suppression was observed for the *its3-1 inp53Δ* mutant (Fig. 2B), consistent with the parallel functions of Syj1 and Inp53 in countering Its3 activity.

To extend this analysis, we tested whether the reduced levels of PI(4,5)P_2 in the *its3-1* mutant might suppress the synthetic-lethal interaction of *inp53Δ* with *pil1Δ* and *syj1Δ*. Strikingly, the triple mutant *its3-1 syj1Δ inp53Δ* was viable at 25℃, but the double

A

	Synthetic Lethals	Correlating Mutants
pil1Δ	*inp53Δ* *whi2Δ* *arv1Δ*	*sle1Δ* *syj1Δ* *tax4Δ*
sle1Δ	*inp53Δ* *whi2Δ* *arv1Δ*	*pil1Δ* *syj1Δ* *tax4Δ*

B

Gene	Description
inp53	5′ phosphatase for PI(4,5)P_2
syj1	polyphosphoinositide phosphatase for PI(4,5)P_2
tax4	ENTH/VHS protein, Syj1 ligand

C

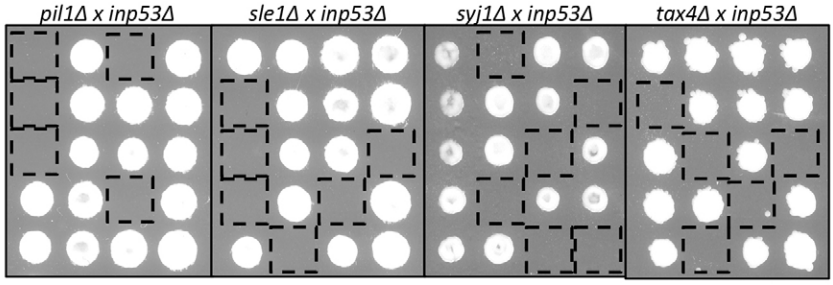

Fig. 1. Genetic interactions identified by synthetic genetic array screens. (A) Summary of genetic interaction results for *pil1Δ* and *sle1Δ*; the table is limited to shared hits that were verified by tetrad dissection. (B) Description of key genes in Pil1-Sle1 genetic interaction screens. (C) Tetrad analysis confirms that *pil1Δ*, *sle1Δ*, *syj1Δ*, and *tax4Δ* are all synthetically lethal with *inp53Δ*. Inviable spores represented by dashed black squares; replica plating showed that inviable spores are the double mutants.

Journal of Cell Science (2014) 127, 1318–1326 doi:10.1242/jcs.143545

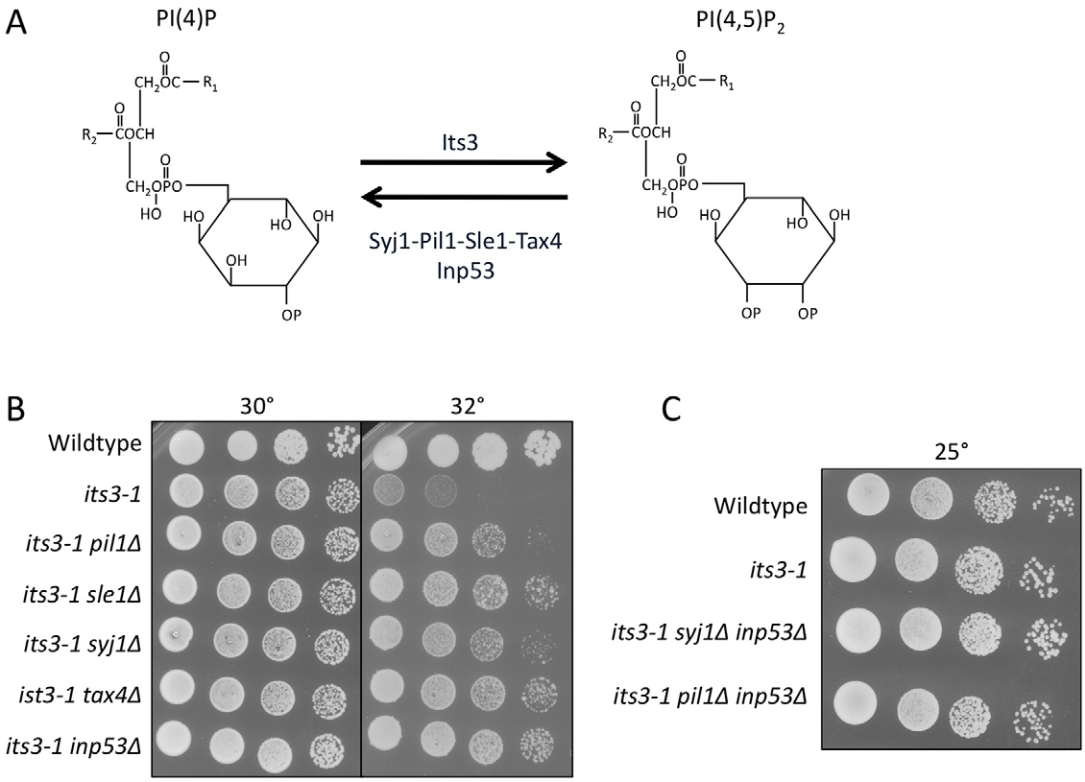

Fig. 2. Eisosomes function in a genetic pathway for PI(4,5)P_2 regulation. (A) Regulation of PI(4,5)P_2 synthesis and hydrolysis in fission yeast. (B) Mutations in the Pil1–Sle1–Syj1–Tax4 pathway suppress temperature-sensitive growth defects of *its3-1*. (C) *its3-1* suppresses the synthetic lethality of *inp53Δ pil1Δ* and *inp53Δ syj1Δ* mutants. Panels B and C are 10-fold serial dilutions grown at the indicated temperatures on rich media.

mutant *syj1Δ inp53Δ* was dead (Fig. 2C). Similarly, *its3-1* suppressed the synthetic lethality of *inp53Δ* with *pil1Δ* (Fig. 2C). We conclude that defects in PI(4,5)P_2 levels underlie the synthetic lethality of *inp53Δ* with both *syj1Δ* and *pil1Δ*. Our combined genetic data link eisosomes with the conversion of PI(4,5)P_2 to PI(4)P through a Pil1–Sle1–Syj1–Tax4 pathway that functions in parallel to Inp53.

Eisosomes require PI(4,5)P_2 dynamics

The functional link between eisosomes and PI(4,5)P_2 led us to examine these structures in mutants that alter PI(4,5)P_2 regulation. In *syj1Δ* cells, Pil1 filaments appeared as spots, and these cells contained higher levels of cytoplasmic Pil1 than wild-type cells (Fig. 3A). This indicates that Syj1 is required for proper eisosome organization. By contrast, we did not detect eisosome defects in *inp53Δ* cells (Fig. 3A), indicating a specific role for Syj1. We also observed eisosome defects in the temperature-sensitive *its3-1* mutant (Fig. 3B), which reduces cellular levels of PI(4,5)P_2 (Mitra et al., 2004). At the permissive temperature of 25℃, cytoplasmic levels of Pil1 were modestly increased in this mutant (Fig. 3B). This defect was more dramatic after 10 minutes at the non-permissive temperature of 32℃ (Fig. 3B,C). We conclude that eisosome organization requires both Syj1 and Its3. This requirement is a conserved feature of eisosomes as budding yeast eisosomes are defective in mutants of either phosphatidylinositol 5-kinase (PI5K) or synaptojanin (Karotki et al., 2011).

The requirement of both Syj1 and Its3, which have opposing functions in PI(4,5)P_2 metabolism, led us to examine eisosomes in *syj1Δ its3-1* double-mutant cells. One possibility was that combining these counteracting mutations might suppress the defects observed in each single mutant. In contrast to this prediction, *syj1Δ its3-1* double-mutant cells displayed unusually thick Pil1 filaments at the cell cortex (Fig. 4A). We used thin-section electron microscopy to investigate the ultrastructure of these thick filaments. In cross-section views, *syj1Δ its3-1* double-mutant cells displayed exaggerated pit-like invaginations that were not observed in either single-mutant or wild-type cells (Figs 4B; supplementary material Fig. S2). Formation of these pits was abolished by deletion of Pil1 as they were not observed in any *pil1Δ syj1Δ its3-1* triple-mutant cells (supplementary material Fig. S2). We conclude that proper eisosome assembly requires the dynamic generation and hydrolysis of PI(4,5)P_2 by Its3 and Syj1. When this cycle is disrupted, Pil1-dependent pits assemble and deform the cell cortex.

Purified Pil1 binds and tubulates liposomes

Our genetic and microscopy results linking eisosomes with PI(4,5)P_2 regulation led us to test the physical interaction of Pil1 with lipids. In liposome-pelleting assays, Pil1 bound modestly to liposomes containing a combination of phosphatidylcholine (PC), phosphatidylserine (PS) and phosphatidylenolamine (PE) (Fig. 5A). This binding was strongly enhanced by the addition of PI(4,5)P_2 (Fig. 5A). We next used negative-stain electron microscopy to visualize Pil1-bound liposomes. Pil1 deformed liposomes and induced the formation of long lipid tubules (Fig. 5B), similar to the liposome-tubulation activity reported for budding yeast Pil1 (Karotki et al., 2011; Olivera-Couto et al., 2011). Similar to the pelleting assays, PI(4,5)P_2 increased the fraction of liposomes tubulated by fission yeast Pil1 [13.3%±3.5%

Journal of Cell Science (2014) 127, 1318–1326 doi:10.1242/jcs.143545

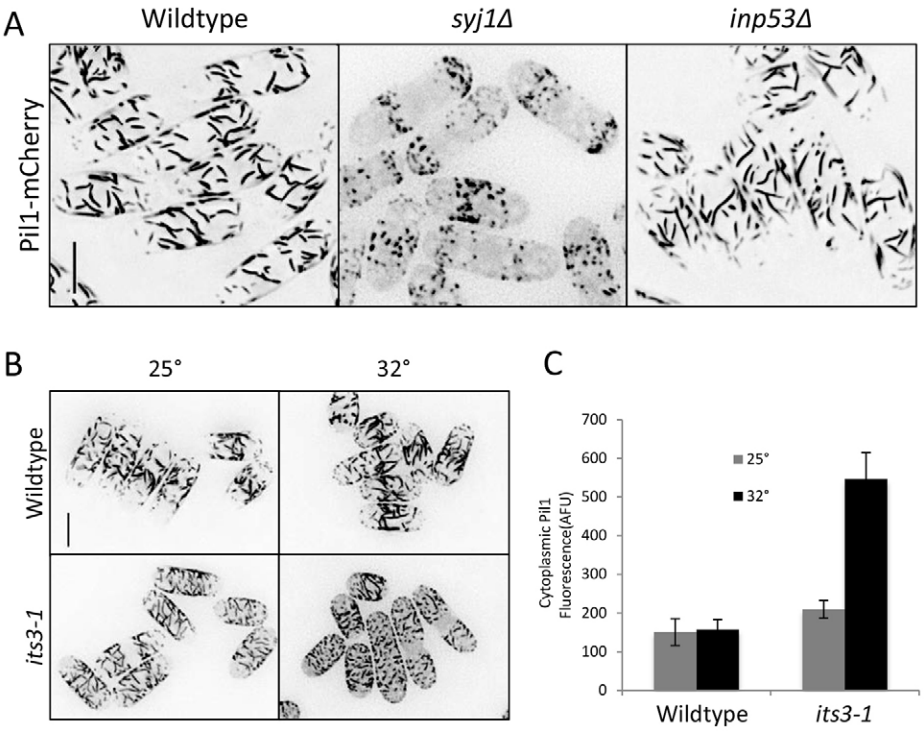

Fig. 3. Eisosome defects in *syj1* and *its3* mutants. (A) Pil1 cortical filaments are dependent on Syj1 but not Inp53 for proper organization. Images are inverted maximum projections for *Z*-planes in the top half of the cell. Scale bar: 5 µm. (B) Eisosome organization is dependent on Its3. Cells were grown at 25°C and then switched to 32°C for 10 minutes. Images are inverted maximum projections from *Z*-planes in the top half of the cell. Scale bar, 5 µm. (C) Quantification of Pil1 cytoplasmic concentration in the indicated strain and temperature. Levels are presented as arbitrary fluorescence units (AFU) and represent mean ± s.d. for 25 cells.

without $PI(4,5)P_2$; 39.8%±4.0% with $PI(4,5)P_2$]. We conclude that Pil1, like other BAR domain proteins, binds to and tubulates membranes containing $PI(4,5)P_2$. This biochemical interaction likely contributes to the regulation of $PI(4,5)P_2$ by the Pil1–Sle1–Syj1–Tax4 pathway.

Given the functional and physical links between Pil1 and $PI(4,5)P_2$, we wondered how Pil1 bound, albeit more modestly, to liposomes that lack this negatively charged lipid. Our liposome preparations contained the negatively charged lipid PS. To test the role of PS, we generated liposomes containing only PC. Pil1 did not pellet with PC liposomes but strongly pelleted upon addition of $PI(4,5)P_2$ (Fig. 5C). Furthermore, Pil1 only tubulated PC liposomes containing $PI(4,5)P_2$ (Fig. 5D). We conclude that Pil1 binds to negatively charged lipids such as PS and displays a strong interaction with $PI(4,5)P_2$. These combined results indicate that Pil1 preferentially alters the geometry of membranes containing $PI(4,5)P_2$, and also functions with synaptojanin to regulate $PI(4,5)P_2$ in cells.

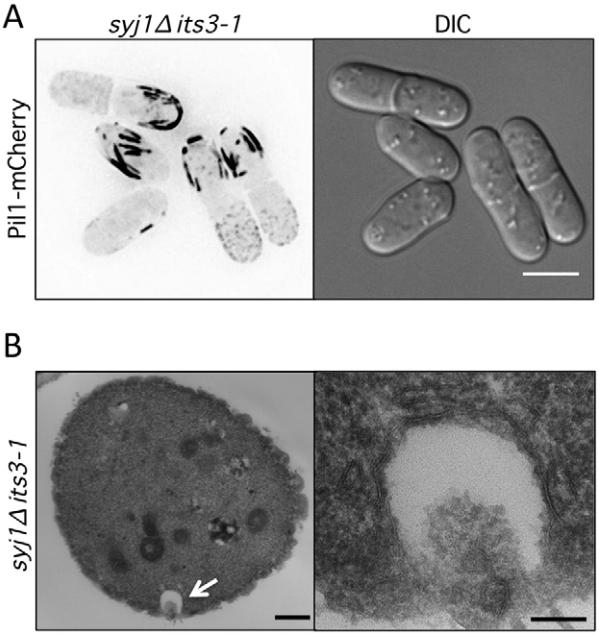

Fig. 4. Pil1 generates cortical pits in *syj1Δ its3-1* double-mutant cells. (A) Thick Pil1 filaments at the cortex of *syj1Δ its3-1* double-mutant cells. Images are inverted maximum projections from *Z*-planes in the top half of the cell. Scale bar, 5 µm. (B) Thin section electron microscopy of *syj1Δ its3-1* double-mutant cells. Cross-section view displays exaggerated pit-like invagination. The white arrow highlights a pit-like invagination that is magnified in right panel. Scale bars: 500 nm (left panel); 100 nm (right panel).

Syj1 and Inp53 are spatially separated in cells

Our genetic results identified two parallel pathways for $PI(4,5)P_2$ hydrolysis, by Inp53 and by Syj1, which acts in the Pil1–Sle1–Syj1–Tax4 pathway. This raises the question how these two lipid phosphatases might be differentially regulated in cells. As a first step to understand their differences, we examined the subcellular localization of Syj1 and Inp53 by fluorescence microscopy (Fig. 6A). Both endogenous gene products were tagged at the C-terminus with monomeric enhanced GFP (mEGFP), and genetic interactions verified that both Syj1–mEGFP and Inp53–mEGFP were functional (supplementary material Fig. S3 and data not shown). Syj1–mEGFP was concentrated in cytoplasmic puncta, as well as in small patches throughout the cell cortex. Inp53–mEGFP localized to cortical patches at growing cell tips and the cell division site. Syj1 localization was not altered in *inp53Δ* cells, and Inp53 puncta were not altered in *syj1Δ* cells (supplementary material Fig. S3). Thus, these functionally overlapping lipid phosphatases localize to independent sites in cells.

Journal of Cell Science (2014) 127, 1318–1326 doi:10.1242/jcs.143545

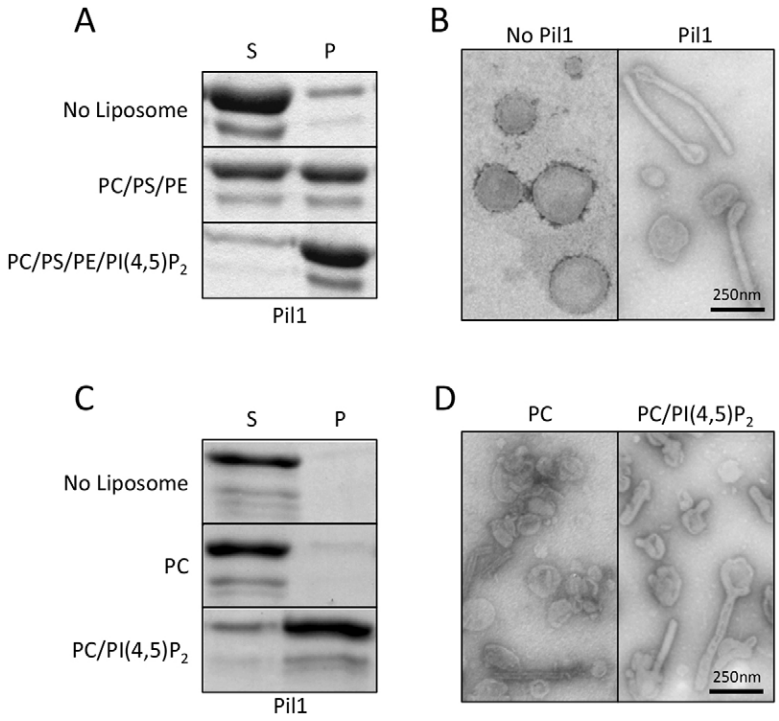

Fig. 5. Pil1 binds and tubulates liposomes *in vitro*. (A) Liposome pelleting assays. Pil1 was incubated with the indicated liposomes, and supernatant (S) and pellet (P) fractions were analyzed by SDS-PAGE followed by Coomassie staining. (B) Electron microscopy of negative-stained lipososomes containing PC/PS/PE/PI(4,5)$_2$ in the presence or absence of purified Pil1. (C) Liposome pelleting assays. Pil1 was incubated with PC liposomes in the presence or absence of 1.5% PI(4,5)P_2, and samples were analyzed as in panel A. (D) Electron microscopy of negative-stained samples from panel C.

We next tested how the localization of Inp53 and Syj1 relates to eisosomes. Fission yeast eisosomes are static filaments restricted to the non-growing regions of the plasma membrane (Kabeche et al., 2011; Snaith et al., 2011). We did not detect colocalization between the eisosome marker Pil1–mCherry and Inp53–mEGFP (Fig. 6B), and Inp53–mEGFP localization was unchanged in *pil1Δ* cells that do not contain eisosomes (supplementary material Fig. S3). This indicates that Inp53 and Pil1 localize independently to distinct structures, consistent with their function in separable genetic pathways. Syj1-mEGFP localizes primarily to cytoplasmic aggregates that do not colocalize with cortical eisosomes (Fig. 6C). This lack of colocalization is most apparent in single-focal-plane images, where Pil1–mCherry is restricted to the cell cortex (Fig. 6C). In addition to cytoplasmic aggregates, Syj1–mEGFP was present at lower levels at transient cortical puncta, which were often found in the center of the cell (Fig. 6C, arrows). These puncta have the potential to colocalize with eisosomes, but further characterization was limited by signal and resolution.

Some cortical puncta of Syj1 appear at cell tips, unlike eisosomes. Similarly, Inp53 localizes almost exclusively to patches at growing cell tips. These patches resembled endocytic actin patches, so we performed colocalization experiments using the actin-patch marker Fim1. Inp53–mEGFP patches all colocalized with Fim1–mCherry, confirming that Inp53 localizes to endocytic actin patches (Fig. 7A). In contrast, Syj1–mEGFP cortical patches largely did not colocalize with Fim1–mCherry (Fig. 7B), although we detected rare instances of colocalization between Syj1–mEGFP and an independent actin-patch marker, Crn1–mCherry (supplementary material Fig. S3). This suggests that most Syj1 cortical puncta are not endocytic actin patches, but rather might represent interactions with eisosomes and other cortical structures. We conclude that Inp53 localizes to endocytic actin patches, but Syj1 localizes to additional structures at the cell cortex and cytoplasm.

The Pil1–Sle1–Syj1–Tax4 pathway antagonizes TORC2 signaling

Inp53 localizes specifically to actin patches, suggesting that it functions exclusively for endocytosis. By contrast, Syj1 localizes to additional cellular structures and functions with eisosomes, which are independent of endocytosis and actin patches (Brach et al., 2011). What then is the role of the Pil1–Sle1–Syj1–Tax4 pathway? In budding yeast, mutations in the TORC2 signaling complex are suppressed by *syj1Δ* but not by *inp53Δ* (Morales-Johansson et al., 2004). This suggests the possibility of a functional separation, whereby Syj1 activity controls signal transduction pathways, whereas Inp53 activity functions in endocytosis. We tested the possibility that the Pil1–Sle1–Syj1–Tax4 pathway connects with TORC2 signaling by combining these mutants with mutations in the TORC2 protein Tor1. In fission yeast, Tor1 is the catalytic subunit of the TORC2 complex, whereas Tor2 is the catalytic subunit of the TORC1 complex. Owing to rapid accumulation of suppressor mutations in *tor1Δ* strains, we used the temperature-sensitive *tor1-L2045D* mutant. These *tor1-L2045D* mutant cells are viable at 25℃ and dead at 37℃ (Ikai et al., 2011). Strikingly, we found that *pil1Δ*, *sle1Δ*, *syj1Δ*, and *tax4Δ* all suppressed the growth defects of *tor1-L2045D* cells at the non-permissive temperature. This suppression is largely specific to the Pil1–Sle1–Syj1–Tax4 pathway because *inp53Δ* provided markedly reduced suppression of the temperature-sensitive *tor1-L2045D* mutant (Fig. 8A). At high temperatures, *tor1-L2045D* mutant cells become multi-septated and branched. Mutations in components of the Pil1–Sle1–Syj1–Tax4 pathway suppressed these defects as the double-mutant cells maintained a cylindrical shape similar to wild-type cells (Fig. 8B). Consistent with these results, we found that mutations in components of the Pil1–Sle1–Syj1–Tax4 pathway suppressed the growth defects of *tor1Δ* cells (supplementary material Fig. S4). These data indicate that regulation of PI(4,5)P_2 by Pil1–Sle1–Syj1–Tax4 feeds into cell signaling pathways that intersect with TORC2.

Journal of Cell Science (2014) 127, 1318–1326 doi:10.1242/jcs.143545

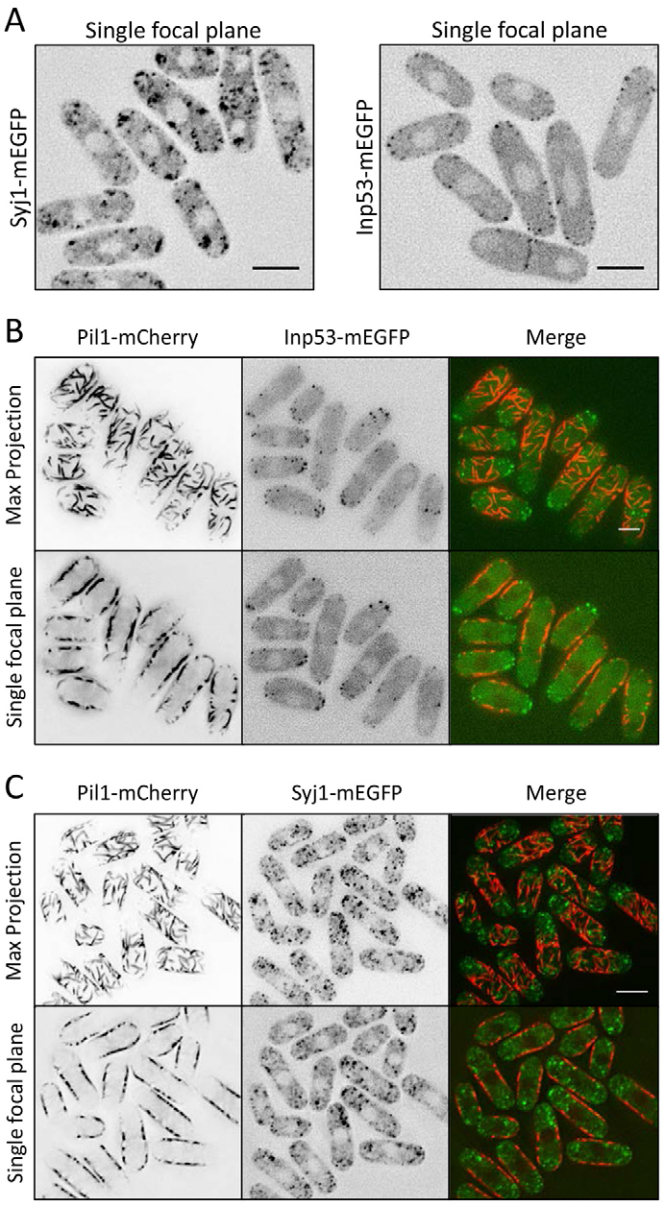

Fig. 6. Syj1 and Inp53 are spatially separated in cells. (A) Localization of endogenously tagged Syj1–mEGFP and Inp53–mEGFP. Images are inverted single focal planes from the cell middle. (B) Inp53–mEGFP does not colocalize with eisosomes, marked by Pil1–mCherry. (C) Most Syj1–mEGFP does not colocalize with eisosomes, marked by Pil1–mCherry. Arrows mark cortical puncta of Syj1–mEGFP. Images in B and C are inverted maximum projections from *Z*-planes in the top half of the cell, and also single focal planes from the cell middle. Scale bars: 5 µm.

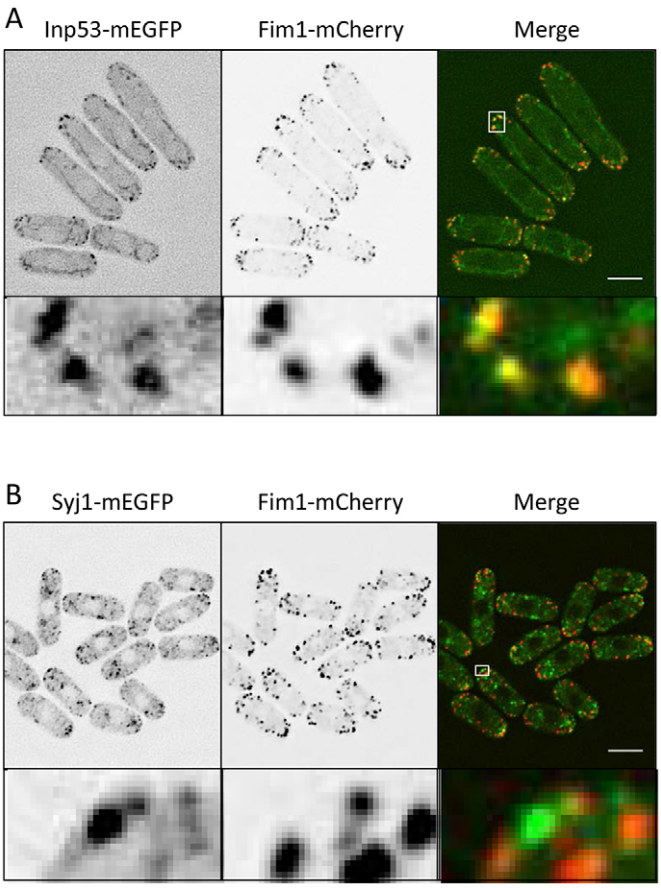

Fig. 7. Inp53 localizes to endocytic actin patches. (A) Colocalization of Inp53–mEGFP and Fim1–mCherry in actin patches; the region boxed in white is magnified in the bottom row. Images are inverted single focal planes. (B) Syj1–mEGFP does not colocalize with actin patches, marked by Fim1–mCherry; the region boxed in white is magnified in the bottom row. Images are inverted single focal planes. Scale bars, 5 µm.

DISCUSSION

A long-standing goal of cell biologists is to connect subcellular structures to cell physiology. In yeast cells, prominent invaginations at the plasma membrane are formed by a cytoplasmic structure called ‘the eisosome’. The membrane-binding protein Pil1 is the core component of eisosomes, and one of the most abundant proteins in a yeast cell. Using an unbiased genetic interaction mapping strategy (Roguev et al., 2007), we have identified a functional genetic pathway for these enigmatic intracellular structures. Our screens showed that the eisosome proteins Pil1 and Sle1 function together with the synaptojanin-like lipid phosphatase Syj1 and its ligand Tax4. Previous work in budding yeast has suggested a genetic connection between Pil1 and Sjl1/Inp51 (Aguilar et al., 2010; Karotki et al., 2011), and our work supports and extends this conserved genetic pathway to include Sle1 and Tax4.

The function of eisosomes has not been elucidated in previous studies because eisosome mutants display no obvious phenotypes in budding yeast or fission yeast. Here, we have shown that eisosomes are essential for cell viability in the absence of the second synaptojanin-like lipid phosphatase Inp53. This provides a context in which to investigate the cellular function of these prominent structures. The additional genetic interactions that we have uncovered between eisosomes and the PI5K mutant *its3-1* identify a role for this pathway in regulating PI(4,5)P_2. Eisosomes perform this cellular function along with Syj1 as part of the Pil1–Sle1–Syj1–Tax4 pathway. Based on these genetic interactions, we propose that the Pil1–Sle1–Syj1–Tax4 pathway functions in parallel to Inp53 to regulate cellular PI(4,5)P_2. The biochemical mechanism that links the activity of Pil1 and Sle1 at eisosomes with the lipid phosphatase activity of Syj1 is unknown. However, we note that the enzymatic activity of synaptojanin proteins is regulated by membrane curvature (Chang-Ileto et al., 2011), and Pil1 generates membrane curvature both at eisosomes in cells and

Journal of Cell Science (2014) 127, 1318–1326 doi:10.1242/jcs.143545

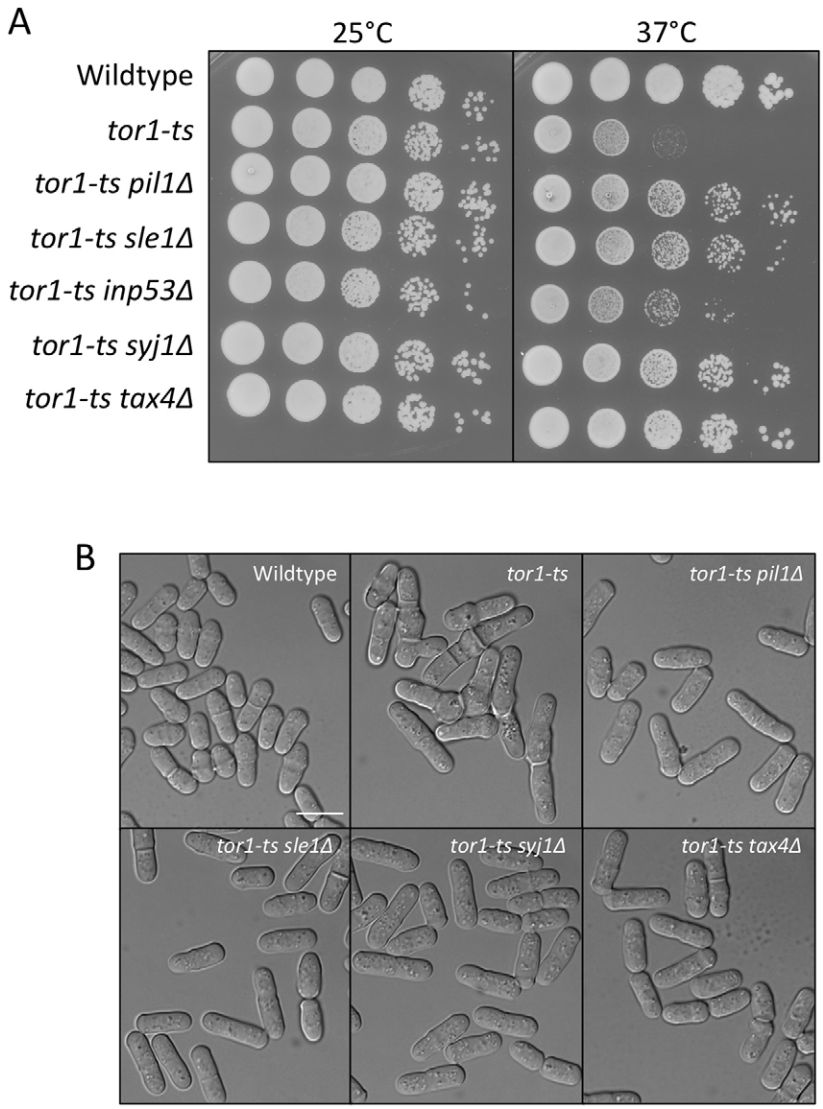

Fig. 8. Pil1–Sle1–Syj1–Tax4 pathway regulates TORC2 signaling. (A) 10-fold serial dilutions of the indicated *tor1-ts* single- and double-mutant cells at different temperatures. Note that temperature-sensitive growth of *tor1-ts* is suppressed by mutations in components of the Pil1–Sle1–Syj1–Tax4 pathway. (B) Digital interference contrast (DIC) images of *tor1-ts* single- and double-mutant cells. Cells were grown for 13 hours at 34˚C. Scale bar, 10 µm.

on liposomes *in vitro*. Thus, an important next step will be to determine the role of Pil1-mediated membrane curvature on Syj1 lipid phosphatase activity both *in vitro* and in cells, as well as to determine the specific regulatory roles of Sle1 and Tax4. In this manner, eisosomes could serve as an experimental paradigm for the mechanisms that connect membrane curvature with lipid composition in a range of cellular contexts.

Our findings have implications for the functional specialization of different $PI(4,5)P_2$ phosphatases in cells. The results of our genetic screens led us to examine the different cellular functions of two related $PI(4,5)P_2$ phosphatases: Syj1 and Inp53. We found that Inp53 localizes to cortical actin patches, where it likely functions in endocytosis. By contrast, Syj1 localizes to different structures in the cytoplasm and cortex. Our work suggests that Syj1 functions with eisosomes to control $PI(4,5)P_2$ levels, with consequences for signal transduction pathways that connect to TORC2. Specifically, we found that mutations in the Pil1–Sle1–Syj1–Tax4 pathway suppress *tor1* mutant phenotypes, indicating that eisosomes are toxic structures when TORC2 signaling is impaired. A likely explanation for this suppression is that $PI(4,5)P_2$ regulation by eisosomes controls a second signaling pathway that cross-talks with TORC2. A prime candidate is the cell-integrity pathway, which senses and relays cell stress through MAP kinase signaling (Levin, 2011; Pérez and Cansado, 2010). In budding yeast, activation of the cell- integrity pathway suppresses TORC2 mutations (Helliwell et al., 1998; Schmidt et al., 1997; Schmidt et al., 1996; Torres et al., 2002). Interestingly, mutations in the budding yeast orthologs of Syj1 and Tax4 activate the cell integrity pathway to suppress TORC2 mutations (Morales-Johansson et al., 2004). We have shown that Syj1 and Tax4 function with eisosomes, and all mutations in this Pil1–Sle1–Syj1–Tax4 pathway can suppress TORC2 mutants in fission yeast. Despite extensive genetic interactions in previous budding yeast studies, the mechanism by which the activation of cell integrity signaling can suppress TORC2 mutants is unclear. Our data indicate that regulation of $PI(4,5)P_2$ by eisosomes might act as an upstream signal in cell integrity signaling for this suppression.

The half-cylinder structure of eisosomes at the plasma membrane has the potential to sense mechanical stress at the plasma membrane. Indeed, eisosomes have been linked with both the sensing of stress at the plasma membrane and the control of TORC2 in budding yeast, where the Slm1 and Slm2 proteins translocate from eisosomes to TORC2 puncta upon plasma

membrane stress (Berchtold et al., 2012). Slm1 does not localize to eisosomes in fission yeast (Kabeche et al., 2011), suggesting that the same mechanism is unlikely to operate in these cells. However, fission yeast eisosomes might play a related stress-sensing role that is connected to the PI(4,5)P_2 regulatory function that we have uncovered. We also note that the membrane geometry of eisosomes in yeast cells is similar to caveolae in metazoan cells. The membrane invaginations at caveolae are proposed to act as membrane reservoirs for rapid cortical expansion upon stress (Mayor, 2011; Sinha et al., 2011). Eisosomes might provide an analogous buffer in fungal species, which lack caveolae. The mechanisms underlying both eisosome and caveolae function require additional work, but their similarities point to the evolution of common design principles for cortical structures in divergent cell types.

MATERIALS AND METHODS

Yeast strains and methods

Standard *S. pombe* media and methods were used (Moreno et al., 1991), and strains used in this study are listed in supplementary material Table S2. Gene tagging and deletion were performed using PCR and homologous recombination (Bähler et al., 1998), and integrations were verified by colony PCR. We confirmed that Syj1–mEGFP and Inp53–mEGFP are functional by assessing the viability of both Syj1–mEGFP *inp53Δ* and Inp53–mEGFP *syj1Δ* strains. All yeast strains were generated by tetrad dissection, when applicable.

The *pombe* epistasis mapper (PEM) system was used for genetic interaction (GI) screening (Roguev et al., 2007). Strains JM1605, JM1606 and JM1613 were crossed to the *S. pombe* deletion collection, and both GI scores and pair-wise correlation coefficients (CC) of GI profiles were generated as described previously (Roguev et al., 2008; Ryan et al., 2012). GI and CC scores for all genetic screens are presented in supplementary material Table S1.

Microscopy

For Fig. 3A; Fig. 4A; Fig. 6; Fig. 7; Fig. 8B and supplementary material Fig. S3, cells were imaged in liquid medium under a coverslip with 0.5 µm step-size using a Deltavision Imaging System (Applied Precision), comprising a customized Olympus IX-71 inverted wide-field microscope, a Photometrics CoolSNAP HQ2 camera, and Insight solid-state illumination unit. Images were captured as *Z*-series and processed by iterative deconvolution in SoftWoRx (Applied Precision), and then analyzed in ImageJ (National Institutes of Health). Maximum intensity projections were generated using five to six focal planes from the top to the middle of the *Z*-series.

For Fig. 3B, cells were imaged on agar pads by spinning disk confocal microscopy on a Nikon Eclipse Ti equipped with a Yokogawa spinning disk, a Nikon ×1001.4NA Plan Apo VC objective, and a Hamamatsu ImagEM C9100-13 EM-CCD camera. This system was controlled by MetaMorph 7 and assembled by Quorum Technologies. Pil1–mCherry and *its3-1* Pil1–mCherry cells were imaged under identical conditions. The mCherry intensity in the cytoplasm (14 pixel×14 pixel box) was measured, and the background signal was subtracted. Quantification was done in ImageJ (National Institutes of Health) and the data shown represent the mean result ± s.d. for 25 cells.

For supplementary material Fig. S2B, germinated cells were imaged directly on YE4S plates using a PixelLINK System, comprising a Zeiss Axioskop 40 and a Mexapixel Fire Wire PL-A661 Camera. Images were captured using PixelLINK Capture SE Software. After imaging, plates were further incubated at 32℃ for determination of genotype by replica plating.

Protein purification

Recombinant Pil1 was purified using the plasmid pJM503 (pGEX6P1–pil1). The plasmid was transformed into *E. coli* strain BL21(DE3). Cells were grown with shaking to an OD_{600} of 0.3 at 37℃, and then shifted to 25℃ for 1 hour before induction by addition of isopropyl β-D-1-thiogalactopyranoside (IPTG). Cells were grown for an additional 4 hours at 25℃ and then harvested by centrifugation, washed into lysis buffer [20 mM HEPES (pH 7.4), 1 mM EDTA, 1 mM dithiothreitol (DTT), 250 mM NaCl, 5% glycerol, Roche complete protease inhibitors (1 tablet per 10 ml cell extract), and 1 mM PMSF, and lysed by French press. The lysate was clarified by centrifugation (15,000 ***g***, 20 min, 4℃), and the resulting supernatant was incubated with glutathione–agarose (Sigma-Aldrich) for 1.5 hours at 4℃. Beads containing GST–Pil1 were washed extensively, and Pil1 was cleaved from GST by overnight incubation with 3C protease. Cleaved Pil1 was verified by SDS-PAGE with Coomassie staining, and dialyzed overnight against a solution containing 20 mM HEPES (pH 7.4), 100 mM NaCl and 5% glycerol. Purified Pil1 migrates as a doublet by SDS-PAGE as shown previously in *S. pombe* and similar to *Sc*Pil1 (Kabeche et al., 2011; Olivera-Couto et al., 2011).

Liposome preparation

Lipids were combined in mixtures comprising PC/PS/PE/Rhodamine–PE (70%/15%/14.5%/0.5%) or, in addition, 1.5% PI(4,5)P_2 (Avanti Polar Lipids) in glass vials and dried under a nitrogen stream. Lipid films were further dried under vacuum for 3 h, then rehydrated at 37℃ in liposome buffer [25 mM HEPES pH 7.4, 150 mM KCl, 2 mM EGTA, 10% glycerol (vol/vol)] for 1 h. To obtain unilamellar vesicles, lipids were subjected to 10 cycles of freeze-thaw and extruded through a polycarbonate filter of 200nm pore size (GE Healthcare) using a mini-extruder (Avanti Polar Lipids).

Pelleting assay

For pelleting assays, Pil1 at 3 µM was incubated in the presence or absence of 10 mM liposomes at room temperature (RT) for 20 min. Samples were centrifuged with an OptimaTXL ultracentrifuge (Beckman) using a TLA-100 rotor at 74,090 ***g*** at 4℃ for 30 min. Supernatants and pellets were collected, adjusted to equal volumes, and analyzed by SDS-PAGE and Coomassie staining.

Electron microscopy

For negative staining, 50 µl drops of liposome with or without Pil1 were spread onto carbon-coated 300-mesh Cu grids (Electron Microscopy Science). After 4 min, excess solution was removed with filter paper, and samples were stained with 2% aqueous uranyl acetate for 2 min. The excess uranyl acetate was removed with filter paper.

For thin sectioning, cells were grown overnight at 25℃ in EMM4S. Cells were pelleted and fixed 1:1 in 5% glutaraldehyde (GTA), 1% paraformaldehyde (PFA) for 15 minutes at RT, then centrifuged at 845 ***g*** for 1 min. Supernatant was removed before cells were fixed in 3% GTA at 10–15 times the volume of the pellet, 1% PFA and 0.1% tannic acid (TA) in 0.1 M sodium cacodylate buffer, pH 7.2–7.4 (NaCac buffer) for 2 h at RT with swirling of sample every 15 min. The fixative was replaced, then cells were incubated one more hour at RT, followed by overnight incubation in fixative on a rotator at 4℃. Cells were subsequently rinsed in PBS and resuspended in 1 ml of Solution A (100 mM KPO_4, pH 7.5, 1.2 M sorbitol and 0.50 µg/ml zymolyase), then incubated with gentle rotation at RT (20 min or 50 min). Cells were washed in Solution A, centrifuged at 845 ***g*** for 1 min, then spun down and washed twice in 2.5% GTA, 1% PFA in 40 mM KPO_4 (pH 6.5–6.7). Cells were then refixed in 3% GTA, 1% PFA, 0.1% TA in NaCac buffer for 2 h at RT, swirling every 15 min. Fix was replaced, and cells rotated overnight at 4℃. Cells were spun at 304 ***g*** for 2 min and washed several times in 0.1 M NaCac (pH 7.2–7.4) over 2 h. Cells were then resuspended in 2% OsO_4 in 0.1 M NaCac (pH 7.2–7.4) for 2 h at RT, swirling every 15 min. Cells were rinsed twice in dH_2O and stained en bloc with 1% aqueous uranyl acetate in dH_2O for 1–2 h at RT in the dark. Cells were dehydrated through ethanol series (30%, 50%, 70%) for 30 min each on a rotator at RT, then rotated for 1–2 days at 4℃. Cells were dehydrated in 85% then 95% ethanol, for 30 min each on a rotator at RT. Cells were then further dehydrated in 100% ethanol on a rotator, using six rinses over 6 h. Cells were then left in 100% ethanol 36–48 h, without rotation, at 4–6℃ to increase infiltration of solutions. Samples were washed in propylene oxide (PO) at RT twice for 30 min and then embedded in epon (LX112 kit; Ladd). Samples were immersed several

times in 1:1 LX112/PO for 3 h on rotator at RT, then 1.5:1 LX112/PO with 4–5 changes over 8 h on a rotator. Samples were placed in a vacuum desiccator overnight, then transferred to BEEM capsules, filled with fresh LX112, and returned to the vacuum desiccator overnight. Samples were polymerized at 45℃ for 8 h and then increased to 60℃ for a further 24 h. Thin sections were mounted on carbon-coated 200-mesh Cu grids (Electron Microscopy Science), stained with 2% methanolic uranyl acetate for 10 min and Reynold's lead citrate for 3 min. All TEM images were taken at 100 kV on a JEOL TEM1010 equipped with a XR-41B AMT digital camera and capture engine software (AMTV540; Advanced Microscopy Techniques).

Acknowledgements
We thank members of the Moseley laboratory and the Biochemistry Department for discussions; Mitsuhiro Yanagida, Vladimir Sirotkin, Fred Chang, and Sophie Martin for strains; Charles Barlowe, Amy Gladfelter, and William Wickner for shared equipment; and Michael Zick for technical help. We thank Louisa Howard and Dartmouth EM Facility for the thin sectioning.

Competing interests
The authors declare no competing interests.

Author contributions
All authors designed experiments and edited the paper. A.R. and N.J.K. performed synthetic genetic array experiments, R.K. performed all other experiments. R.K. and J.B.M. wrote the paper.

Funding
This work was funded by National Institutes of Health [grant numbers GM099774 to J.B.M., T32-GM008704 to R.K. and GM084448, GM084279, GM081879 and GM098101 all to N.J.K.]. J.B.M. is a Pew Scholar in the Biomedical Sciences. N.J.K. is a Searle Scholar and a Keck Young Investigator. Deposited in PMC for release after 12 months.

Supplementary material
Supplementary material available online at
http://jcs.biologists.org/lookup/suppl/doi:10.1242/jcs.143545/-/DC1

References
Aguilar, P. S., Fröhlich, F., Rehman, M., Shales, M., Ulitsky, I., Olivera-Couto, A., Braberg, H., Shamir, R., Walter, P., Mann, M. et al. (2010). A plasma-membrane E-MAP reveals links of the eisosome with sphingolipid metabolism and endosomal trafficking. *Nat. Struct. Mol. Biol.* **17**, 901-908.

Bähler, J., Wu, J. Q., Longtine, M. S., Shah, N. G., McKenzie, A., 3rd, Steever, A. B., Wach, A., Philippsen, P. and Pringle, J. R. (1998). Heterologous modules for efficient and versatile PCR-based gene targeting in Schizosaccharomyces pombe. *Yeast* **14**, 943-951.

Beltrao, P., Cagney, G. and Krogan, N. J. (2010). Quantitative genetic interactions reveal biological modularity. *Cell* **141**, 739-745.

Berchtold, D., Piccolis, M., Chiaruttini, N., Riezman, I., Riezman, H., Roux, A., Walther, T. C. and Loewith, R. (2012). Plasma membrane stress induces relocalization of Slm proteins and activation of TORC2 to promote sphingolipid synthesis. *Nat. Cell Biol.* **14**, 542-547.

Brach, T., Specht, T. and Kaksonen, M. (2011). Reassessment of the role of plasma membrane domains in the regulation of vesicular traffic in yeast. *J. Cell Sci.* **124**, 328-337.

Chang-Ileto, B., Frere, S. G., Chan, R. B., Voronov, S. V., Roux, A. and Di Paolo, G. (2011). Synaptojanin 1-mediated PI(4,5)P2 hydrolysis is modulated by membrane curvature and facilitates membrane fission. *Dev. Cell* **20**, 206-218.

Douglas, L. M., Wang, H. X., Li, L. and Konopka, J. B. (2011). Membrane Compartment Occupied by Can1 (MCC) and Eisosome Subdomains of the Fungal Plasma Membrane. *Membranes (Basel)* **1**, 394-411.

Fröhlich, F., Moreira, K., Aguilar, P. S., Hubner, N. C., Mann, M., Walter, P. and Walther, T. C. (2009). A genome-wide screen for genes affecting eisosomes reveals Nce102 function in sphingolipid signaling. *J. Cell Biol.* **185**, 1227-1242.

Grossmann, G., Opekarová, M., Malinsky, J., Weig-Meckl, I. and Tanner, W. (2007). Membrane potential governs lateral segregation of plasma membrane proteins and lipids in yeast. *EMBO J.* **26**, 1-8.

Grossmann, G., Malinsky, J., Stahlschmidt, W., Loibl, M., Weig-Meckl, I., Frommer, W. B., Opekarová, M. and Tanner, W. (2008). Plasma membrane microdomains regulate turnover of transport proteins in yeast. *J. Cell Biol.* **183**, 1075-1088.

Hartman, N. C. and Groves, J. T. (2011). Signaling clusters in the cell membrane. *Curr. Opin. Cell Biol.* **23**, 370-376.

Helliwell, S. B., Schmidt, A., Ohya, Y. and Hall, M. N. (1998). The Rho1 effector Pkc1, but not Bni1, mediates signalling from Tor2 to the actin cytoskeleton. *Curr. Biol.* **8**, 1211-S2.

Ikai, N., Nakazawa, N., Hayashi, T. and Yanagida, M. (2011). The reverse, but coordinated, roles of Tor2 (TORC1) and Tor1 (TORC2) kinases for growth, cell cycle and separase-mediated mitosis in Schizosaccharomyces pombe. *Open Biol.* **1**, 110007.

Kabeche, R., Baldissard, S., Hammond, J., Howard, L. and Moseley, J. B. (2011). The filament-forming protein Pil1 assembles linear eisosomes in fission yeast. *Mol. Biol. Cell* **22**, 4059-4067.

Karotki, L., Huiskonen, J. T., Stefan, C. J., Ziółkowska, N. E., Roth, R., Surma, M. A., Krogan, N. J., Emr, S. D., Heuser, J., Grünewald, K. et al. (2011). Eisosome proteins assemble into a membrane scaffold. *J. Cell Biol.* **195**, 889-902.

Levin, D. E. (2011). Regulation of cell wall biogenesis in Saccharomyces cerevisiae: the cell wall integrity signaling pathway. *Genetics* **189**, 1145-1175.

Lingwood, D. and Simons, K. (2010). Lipid rafts as a membrane-organizing principle. *Science* **327**, 46-50.

Malinska, K., Malinsky, J., Opekarova, M. and Tanner, W. (2004). Distribution of Can1p into stable domains reflects lateral protein segregation within the plasma membrane of living S. cerevisiae cells. *J. Cell Sci.* **117**, 6031-6041.

Marguerat, S., Schmidt, A., Codlin, S., Chen, W., Aebersold, R. and Bähler, J. (2012). Quantitative analysis of fission yeast transcriptomes and proteomes in proliferating and quiescent cells. *Cell* **151**, 671-683.

Mayor, S. (2011). Need tension relief fast? Try caveolae. *Cell* **144**, 323-324.

Mitra, P., Zhang, Y., Rameh, L. E., Ivshina, M. P., McCollum, D., Nunnari, J. J., Hendricks, G. M., Kerr, M. L., Field, S. J., Cantley, L. C. et al. (2004). A novel phosphatidylinositol(3,4,5)P3 pathway in fission yeast. *J. Cell Biol.* **166**, 205-211.

Morales-Johansson, H., Jenoe, P., Cooke, F. T. and Hall, M. N. (2004). Negative regulation of phosphatidylinositol 4,5-bisphosphate levels by the INP51-associated proteins TAX4 and IRS4. *J. Biol. Chem.* **279**, 39604-39610.

Moreira, K. E., Walther, T. C., Aguilar, P. S. and Walter, P. (2009). Pil1 controls eisosome biogenesis. *Mol. Biol. Cell* **20**, 809-818.

Moreira, K. E., Schuck, S., Schrul, B., Fröhlich, F., Moseley, J. B., Walther, T. C. and Walter, P. (2012). Seg1 controls eisosome assembly and shape. *J. Cell Biol.* **198**, 405-420.

Moreno, S., Klar, A. and Nurse, P. (1991). Molecular genetic analysis of fission yeast Schizosaccharomyces pombe. *Methods Enzymol.* **194**, 795-823.

Olivera-Couto, A. and Aguilar, P. S. (2012). Eisosomes and plasma membrane organization. *Mol. Genet. Genomics* **287**, 607-620.

Olivera-Couto, A., Graña, M., Harispe, L. and Aguilar, P. S. (2011). The eisosome core is composed of BAR domain proteins. *Mol. Biol. Cell* **22**, 2360-2372.

Pérez, P. and Cansado, J. (2010). Cell integrity signaling and response to stress in fission yeast. *Curr. Protein Pept. Sci.* **11**, 680-692.

Roguev, A., Wiren, M., Weissman, J. S. and Krogan, N. J. (2007). High-throughput genetic interaction mapping in the fission yeast Schizosaccharomyces pombe. *Nat. Methods* **4**, 861-866.

Roguev, A., Bandyopadhyay, S., Zofall, M., Zhang, K., Fischer, T., Collins, S. R., Qu, H., Shales, M., Park, H. O., Hayles, J. et al. (2008). Conservation and rewiring of functional modules revealed by an epistasis map in fission yeast. *Science* **322**, 405-410.

Ryan, C. J., Roguev, A., Patrick, K., Xu, J., Jahari, H., Tong, Z., Beltrao, P., Shales, M., Qu, H., Collins, S. R. et al. (2012). Hierarchical modularity and the evolution of genetic interactomes across species. *Mol. Cell* **46**, 691-704.

Scazzocchio, C., Vangelatos, I. and Sophianopoulou, V. (2011). Eisosomes and membrane compartments in the ascomycetes: A view from Aspergillus nidulans. *Commun. Integr. Biol.* **4**, 64-68.

Schmidt, A., Kunz, J. and Hall, M. N. (1996). TOR2 is required for organization of the actin cytoskeleton in yeast. *Proc. Natl. Acad. Sci. USA* **93**, 13780-13785.

Schmidt, A., Bickle, M., Beck, T. and Hall, M. N. (1997). The yeast phosphatidylinositol kinase homolog TOR2 activates RHO1 and RHO2 via the exchange factor ROM2. *Cell* **88**, 531-542.

Sinha, B., Köster, D., Ruez, R., Gonnord, P., Bastiani, M., Abankwa, D., Stan, R. V., Butler-Browne, G., Vedie, B., Johannes, L. et al. (2011). Cells respond to mechanical stress by rapid disassembly of caveolae. *Cell* **144**, 402-413.

Snaith, H. A., Thompson, J., Yates, J. R., III and Sawin, K. E. (2011). Characterization of Mug33 reveals complementary roles for actin cable-dependent transport and exocyst regulators in fission yeast exocytosis. *J. Cell Sci.* **124**, 2187-2199.

Strádalová, V., Stahlschmidt, W., Grossmann, G., Blazíková, M., Rachel, R., Tanner, W. and Malinsky, J. (2009). Furrow-like invaginations of the yeast plasma membrane correspond to membrane compartment of Can1. *J. Cell Sci.* **122**, 2887-2894.

Torres, J., Di Como, C. J., Herrero, E. and De La Torre-Ruiz, M. A. (2002). Regulation of the cell integrity pathway by rapamycin-sensitive TOR function in budding yeast. *J. Biol. Chem.* **277**, 43495-43504.

Walther, T. C., Brickner, J. H., Aguilar, P. S., Bernales, S., Pantoja, C. and Walter, P. (2006). Eisosomes mark static sites of endocytosis. *Nature* **439**, 998-1003.

Young, M. E., Karpova, T. S., Brügger, B., Moschenross, D. M., Wang, G. K., Schneiter, R., Wieland, F. T. and Cooper, J. A. (2002). The Sur7p family defines novel cortical domains in Saccharomyces cerevisiae, affects sphingolipid metabolism, and is involved in sporulation. *Mol. Cell. Biol.* **22**, 927-934.

Ziółkowska, N. E., Karotki, L., Rehman, M., Huiskonen, J. T. and Walther, T. C. (2011). Eisosome-driven plasma membrane organization is mediated by BAR domains. *Nat. Struct. Mol. Biol.* **18**, 854-856.

Ziółkowska, N. E., Christiano, R. and Walther, T. C. (2012). Organized living: formation mechanisms and functions of plasma membrane domains in yeast. *Trends Cell Biol.* **22**, 151-158.